

Quadrotor Transporting Cable-Suspended Load using iterative Linear Quadratic Regulator (iLQR) Optimal Control

Yaser Alothman^{1,2}Dongbing Gu¹

Abstract—This paper presents an iterative linear quadratic regulator (iLQR) optimal controller of a high level dynamic model using Euler-Lagrange equations for a single quadrotor UAV with a cable-suspended heavy rigid body. The control algorithm is constructed in order to improve two possible outputs: firstly, precisely tracking a given desired trajectory for a quadrotor with load, and, secondly, considering an anti-swing load through a transporting task. Two challenges have been taken into account: aggressive trajectory tracking and stability in behaviour; these must be guaranteed for the full UAV carrying the payload. The high nonlinear dynamic model of the quadrotor with a consideration of the cable suspended payload is represented in eleven degrees of freedom. Subsequently, the nonlinear dynamic model is linearised in two modes, a vehicle mode without a load effect during a taking-off task and a switching-to-quad-load system mode considering the load effect used in a simulation. The simulation results are presented to illustrate the system stability improvement and precise implementation through verifying the iLQR parameters in comparison with the LQR controller.

I. INTRODUCTION

The demand for Unmanned Aerial Vehicles (UAVs) carrying a payload with a cable has worthily increased in the recent decade. Military and civil applications are commonly investigated in many research areas such as reconnaissance, rescue, construction, firefighting and freight transportation. Transportation of a cable-slung load via a single quadrotor is an influential key task that needs to be considered. However, because the suspended load is heavy and swings during the transportation task in different complex motions, controlling the full nonlinear exemplary model autonomously is complicated. Furthermore, the high nonlinearities and uncertainties of the quadrotor and suspended load make the system unstable during the transportation in rough circumstances. Therefore, safe transportation task includes taking off, following a trajectory and landing in safe control and minimum fluctuation. Ideally, this will prevent dangerous behaviour and damage for the quadrotor through transportation. *investigated?*

Different types of controllers have been investigated to control the quadrotor with a suspended load. For instance, Sadr et al.[1] relied on an anti-swing algorithm and designed a nonlinear controller for a dynamic model system in order to control the position and attitude of a quadrotor with a slung load, while a nonlinear control technique for the dynamic

model of the quadrotor with slung load trajectory tracking and stabilisation was proposed in [2]. A backstepping controller was presented for a payload connected with the quadrotors center of gravity. Kanes method was modeled for trajectory tracking and for verifying the simulation results [3]. A Non-linear Model Predictive Control (NMPC) was proposed by [4] to track waypoints precisely and restrain large oscillations for the slung load actively, and it was then compared with the performance of a LQR controller to improve the simulation results considering aggressive maneuvers. While in [5], flight system architecture and software were presented to test a nonlinear model predictive controller (NMPC) to track both the load and the quadrotor for a safe and precise transportation of a heavy load.

A dynamic model was developed based on the Udwadia-Kalaba equations for a slung load lifted by a quadrotor in [6], where an appropriate neural network and an adaptive control were proposed to develop attitude and numerical simulations were performed. A hybrid dynamical system was modeled in [7] to navigate a quadrotor with a slung load in known obstacle environments within two challenges: the full system had to, firstly, guarantee obstacle avoidance, and, secondly, give a permission for maneuvers through adaptation between subsystems. A complex controller was designed in [8] based on the least-square estimation and the geometric combination control in order to transport the load from one point to another. Moreover, in [9] a combination of adaptive design and neural network controllers were developed to overcome of unmodeled dynamic effects.

Linear controllers are another type applied to solve the problem of the quadrotor with a suspended load control. For example, In [10] lifting and transporting a payload was performed for a quadrotor carrying the load with a cable. The proposed controller was LQR control algorithm. Two modes were presented: a starting mode taking off without the load influence then switching to a mode with the effect of the load. The simulation results for the LQR controller were compared with the PD controller results. In [11] an LQR controller was designed for a quadrotor to maintain the position and attitude equilibrium in spite of losing a single propeller, two opposite or even three propellers. A Sequential Linear Quadratic (SLQ) control was presented in [12] and an iterative LQG algorithm (iLQG) was presented in [13] for a hybrid model quadrotor and slung load to perform two approaches. The first was passing through an unfairly high window for the payload pass by

¹School of Computer Science and Electronic Engineering, University of Essex, Wivenhoe Park, Colchester, UK.

Email: ynialo@essex.ac.uk, dgu@essex.ac.uk

²University of Technology, Baghdad-Iraq

implementing aggressive maneuvers. The second demonstrated a go-to-goal task with one and then two rotor failures.

II. CONTRIBUTIONS

In this paper, the general optimal controllers ILQR and LQR are proposed to implement different complex tasks through overcoming the limitations of a nonlinear and unstable system. Furthermore, the performance is improved through comparison between the results of both approaches. However, lifting and transporting tasks are demonstrated in one algorithm implementation using two different system models and a cost function for each. To the best of our knowledge, the unique use of the ILQR algorithm for the transportation of a specific payload hanging from a quadrotor by a flexible cable has not been examined. In the following, Section III presents the precise mathematical model of the quadrotor with a cable suspended load. Section IV illustrates the derivation of the ILQR control approach fundamentals. Section V describes the simulation results. Our conclusion and suggestions for future work are given in Section VI.

III. QUADROTOR WITH SUSPENDED LOAD MODEL

A. Nonlinear Dynamic Model

The full nonlinear system dynamics of a quadrotor and a payload has been derived from a translation-rotation model. The system is subjected to the assumptions such as a symmetrical rigid body of the quadrotor, a point mass load and massless cable. The derivation dynamic of the quadrotor-slung point mass model is demonstrated according to the above assumptions. In order to model full 11 degrees of freedom (DOF), two coordinate reference frames have been defined, an inertial frame (earth fixed frame) denoted by **E** and a rigid body fixed frame denoted by **B**. The coordinate positions are denoted as x_E, y_E, z_E for (EFF) and x_B, y_B, z_B for (BFF), respectively. The attitude of the payload is represented by two spheres, while its position is obtained with respect to the quadrotor position. Symbols and acronyms are listed as:

R	Rotation matrix from inertia frame to body frame
ϕ	Roll angle along x-coordinate of the quadrotor
θ	Pitch angle along y-coordinate of the quadrotor
ψ	Yaw angle along z-coordinate of the quadrotor
ϕ_L	Roll angle along x-coordinate of the suspended load
θ_L	Pitch angle along y-coordinate of the suspended load
$\chi_Q, \chi_L \in R^3$	Positions of the quadrotor center of gravity and load
$v_Q, v_L \in R^3$	Velocity of the quadrotor center of gravity and load
F, M	Total thrust and moment produced by the quadrotor

Ω	Angular velocity of the quadrotor
I	Inertia matrix of the quadrotor
τ	Torque on airframe body
b	Thrust factor
d	Drag factor
L	Cable length
T	Cable tension
m_Q	Mass of the quadrotor
m_p	Mass of the suspended payload
e_1, e_2, e_3	Three coordinate unit vectors
ρ	Unit vector from quadrotor attached point to the load

The system is recognised by the quadrotor location with respect to the inertial frame, the load and the quadrotor attitudes. The cable suspended load carried by the quadrotor is modelled with eight degrees of freedom (DOF) in the case of a nonzero cable, which is comprised of six 6 (DOF) for the quadrotor as a rigid body and two 2 (DOF) for the spherical pendulum load, where the relation between quadrotors and load positions are presented by

$$x_L = x_Q + L\rho$$

The full equations of motion are obtained using the Euler-Lagrange method. The Lagrangian is composed of kinetic energy subtracting potential energy as in the following equation:

$$\mathcal{L} = \mathfrak{T} - \mathfrak{U}$$

while the system kinetic energy \mathfrak{T} is composed of translational and rotational quadrotors and load kinetic energy;

$$\text{动能} \quad \mathfrak{T} = \frac{1}{2}m_Q\dot{x}_Q^2 + \frac{1}{2}m_p\dot{x}_L^2 + \frac{1}{2}\Omega \cdot \mathfrak{J} \cdot \Omega$$

The potential energy is

$$\text{势能} \quad \mathfrak{U} = m_Qg e_3 \cdot x_Q + m_p g e_3 \cdot x_L$$

When the quadrotor starts to take off, the cable tension starts with zero value and the dynamic model is considered as two separate systems: the quadrotor model and the free fall load dynamic model.

Now, in order to improve the switching process to transfer models operation, two conditions are considered: the state condition $m = m_Q + m_L$ and the total mass of the quadrotor and load with neglecting the cable mass. The first and second states are $m = m_Q + \delta_m$ and $z_q < 1 + \delta_z$. If the two conditions are approved depending on the factors δ_m and δ_z , then the zero cable tension model system is used. However, the switching model proceeds to the second non-zero cable tension, where δ_m is a small positive number which represents arbitrary mass change due to additional types of equipment and δ_z is a distortion cable length. The non-zero cable tension

$$\textcolor{red}{M_3 = M_\phi} \quad \textcolor{blue}{M_2 = M_\psi}$$

model is represented as follows [10]:

$$\dot{x}_Q = v_Q \quad (1)$$

$$m_Q \ddot{v}_Q = FRe_3 - m_Q ge_3 - T\rho$$

$$\dot{x}_L = v_L$$

$$m_p \ddot{v}_L = -m_p g e_3 + T\rho$$

$$I\dot{\Omega} = -\Omega \times I\Omega + M$$

where ρ is a unit vector from the quadrotor centre of gravity to the load which represents a cable direction vector in the body frame [8]. The cable tension T is equal to the magnitude of the cable force multiplied by the unit vector ρ [1].

$$T = |f| \rho$$

where the magnitude of the cable forces $|f|$ is

$$|f| = m_L \dot{v}_L. \quad (3)$$

The non-zero cables tension of the nonlinear dynamical model (1)-(2) for leader and follower quadrotors carrying a payload by cables is represented in the following equations:

$$\begin{aligned} \ddot{x}_Q &= (U1(\sin \phi_Q \sin \psi_Q + \cos(\psi_Q) \cos(\phi_Q) \sin(\theta_Q)) \\ &\quad + Lm_p(\sin(\phi_L)(2 \cos(\theta_L)\dot{\phi}_L \dot{\theta}_L + \sin(\theta_L)\ddot{\phi}_L) \\ &\quad + \cos(\phi_L)(\sin(\theta_L)(\dot{\phi}_L^2 + \dot{\theta}_L^2) - \cos(\theta_L)\ddot{\theta}_L)))/(m_Q + m_p) \end{aligned} \quad (4)$$

$$\begin{aligned} \ddot{y}_Q &= (U1(\cos(\phi_Q) \sin(\psi_Q) \sin(\theta_Q) - \sin(\phi_Q) \cos(\psi_Q)) \\ &\quad + L1m_p(-\sin(\phi_L)\dot{\phi}_L^2 + \cos(\phi_L)\ddot{\phi}_L))/(m_Q + m_p) \end{aligned} \quad (5)$$

$$\begin{aligned} \ddot{z}_Q &= (-g(m_Q + m_p) + U1(\cos(\phi_Q) \cos(\theta_Q)) \\ &\quad + Lm_p \sin(\phi_L)(-2 \sin(\theta_L)\dot{\phi}_L \dot{\theta}_L + \cos(\theta_L)\ddot{\phi}_L) \\ &\quad + Lm_p \cos(\phi_L)(\cos(\theta_L)(\dot{\phi}_L^2 + \dot{\theta}_L^2) + \sin(\theta_L)\ddot{\theta}_L))/(m_Q + m_p) \end{aligned} \quad (6)$$

$$(7)$$

$$\ddot{\phi}_Q = \frac{I_{yy} - I_{zz}}{I_{xx}} \dot{\theta}\dot{\psi} - \frac{I_r}{I_{xx}} \dot{\theta}\Omega + \frac{M_\phi}{I_{xx}} \quad (8)$$

$$\ddot{\theta}_Q = \frac{I_{zz} - I_{xx}}{I_{yy}} \dot{\phi}\dot{\psi} - \frac{I_r}{I_{yy}} \dot{\phi}\Omega + \frac{M_\theta}{I_{yy}} \quad (9)$$

$$\ddot{\psi}_Q = \frac{I_{xx} - I_{yy}}{I_{zz}} \dot{\phi}\dot{\theta} + \frac{M_\psi}{I_{zz}} \quad (10)$$

$$(11)$$

$$\begin{aligned} \ddot{x}_L &= \ddot{x}_Q - L * \cos(\phi_L) \sin(\theta_L) \dot{\phi}_L^2 - 2 * L * \sin(\phi_L) \\ &\quad \cos(\theta_L) \dot{\phi}_L \dot{\theta}_L - L * \cos(\phi_L) \sin(\theta_L) \dot{\theta}_L^2 \\ &\quad - L * \sin(\phi_L) \sin(\theta_L) \ddot{\phi}_L + L * \cos(\phi_L) \cos(\theta_L) \ddot{\theta}_L \end{aligned} \quad (12)$$

$$\ddot{y}_L = L * \sin(\phi_L) \dot{\phi}_L^2 - L * \cos(\phi_L) \ddot{\phi}_L + \ddot{y}_Q \quad (13)$$

$$\begin{aligned} \ddot{z}_L &= \ddot{z}_Q - L * \cos(\phi_L) \cos(\theta_L) \dot{\phi}_L^2 + 2 * L * \sin(\phi_L) \\ &\quad \sin(\theta_L) \dot{\phi}_L \dot{\theta}_L - L * \cos(\phi_L) \cos(\theta_L) \dot{\theta}_L^2 - \end{aligned} \quad (14)$$

$$L * \sin(\phi_L) \cos(\theta_L) \ddot{\phi}_L - L * \cos(\phi_L) \sin(\theta_L) \ddot{\theta}_L \quad (15)$$

$$\begin{aligned} \ddot{\phi}_L &= (-U3 + Lm_p(L \cos(\phi_L) \cos(\theta_L)^2 \sin(\phi_L) \\ &\quad (\dot{\phi}_L^2 + \dot{\theta}_L^2) + \sin(\phi_L) \sin(\theta_L) \dot{x}_Q \\ &\quad + \cos(\phi_L)(L \sin(\phi_L)(-(-1 + (\sin(\theta_L))^2)\dot{\phi}_L^2 \\ &\quad - (\sin(\theta_L))^2 \dot{\theta}_L^2) + \ddot{y}_Q) + \cos(\theta_L) \sin(\phi_L) \\ &\quad (g + \ddot{z}_Q)))/(I_{xx} + L^2 m_p) \end{aligned} \quad (16)$$

$$\begin{aligned} \ddot{\theta}_L &= (-U2 + Lm_p * \cos(\phi_L)(\cos(\theta_L)(2L \cos(\theta_L) \sin(\phi_L) \\ &\quad \dot{\phi}_L \dot{\theta}_L - \dot{x}_Q) + \sin(\theta_L)(g + 2L \sin(\phi_L) \sin(\theta_L) \dot{\phi}_L \dot{\theta}_L \\ &\quad + \ddot{z}_Q)))/(I_{yy} + (L_1^2 + L_2^2)m_p \cos(\phi_L)^2). \end{aligned} \quad (17)$$

B. Linearised Model

Linearisation around an operating point is the most important requirement in order to implement the ILQR controller for the mathematical model of a quadrotor with a slung load. Then equations (4)-(17) can be represented in a state space as follows:

$$\dot{X} = AX + BU \quad (18)$$

$$Y = CX + DU \quad (19)$$

where $X = [x, y, z, \phi, \theta, \psi, x_L, y_L, z_L, \phi_L, \theta_L, \dot{x}, \dot{y}, \dot{z}, \dot{\phi}, \dot{\theta}, \dot{\psi}, x'_L, y'_L, z'_L, \phi'_L, \theta'_L]^T$, $U = [F, M_\phi, M_\theta, M_\psi]^T$, $Y = [x, y, z, \psi]$, ← 其他状态变量不可直接输入模型

$$A = \begin{bmatrix} \mathbf{0}_{11 \times 9} & \mathbf{0}_{11 \times 1} & \mathbf{0}_{11 \times 1} & \mathbf{J}_{11 \times 11} \\ \mathbf{0}_{1 \times 9} & \frac{-gL^2 m_p^2}{den1} & 0 & \mathbf{0}_{1 \times 11} \\ \mathbf{0}_{1 \times 9} & 0 & \frac{gL^2 m_p^2}{den2} & \mathbf{0}_{1 \times 11} \\ \mathbf{0}_{4 \times 9} & \mathbf{0}_{4 \times 1} & \mathbf{0}_{4 \times 1} & \mathbf{0}_{4 \times 11} \\ \mathbf{0}_{1 \times 9} & \frac{gL^2 m_p}{den2} & 0 & \mathbf{0}_{1 \times 11} \\ \mathbf{0}_{1 \times 9} & 0 & \frac{-gL^2 m_p}{den1} & \mathbf{0}_{1 \times 11} \\ \mathbf{0}_{1 \times 9} & 0 & 0 & \mathbf{0}_{1 \times 11} \\ \mathbf{0}_{1 \times 9} & \frac{gL^2 m_p (m_p + m_Q)}{den1} & 0 & \mathbf{0}_{1 \times 11} \\ \mathbf{0}_{1 \times 9} & 0 & \frac{gL^2 m_p (m_p + m_Q)}{den2} & \mathbf{0}_{1 \times 11} \end{bmatrix} \quad (20)$$

$$B = \begin{bmatrix} \mathbf{0}_{11 \times 1} & \mathbf{0}_{11 \times 1} & \mathbf{0}_{11 \times 1} & \mathbf{0}_{11 \times 1} \\ 0 & \frac{Lm_p}{den1} & 0 & 0 \\ 0 & 0 & \frac{-Lm_p}{den2} & 0 \\ \frac{1}{(m_Q + m_p)} & 0 & 0 & 0 \\ 0 & \frac{1}{I_{xx}} & 0 & 0 \\ 0 & 0 & \frac{1}{I_{yy}} & 0 \\ 0 & 0 & 0 & \frac{1}{I_{zz}} \\ 0 & \frac{-L*m_q}{den1} & 0 & 0 \\ 0 & 0 & \frac{L*m_q}{den2} & 0 \\ \frac{1}{(m_Q + m_p)} & 0 & 0 & 0 \\ 0 & \frac{(m_p + m_Q)}{den1} & 0 & 0 \\ 0 & 0 & \frac{(m_p + m_Q)}{den2} & 0 \end{bmatrix} \quad (21)$$

where $den1 = (m_p m_Q L^2 + I_{xx}(m_p + m_Q))$ and $den2 = (m_p m_Q L^2 + I_{yy}(m_p + m_Q))$

$$C = \begin{bmatrix} \mathbf{J}_{3 \times 3} & \mathbf{0}_{3 \times 2} & \mathbf{0}_{3 \times 1} & \mathbf{0}_{3 \times 16} \\ \mathbf{0}_{1 \times 3} & \mathbf{0}_{1 \times 2} & 1 & \mathbf{0}_{1 \times 16} \end{bmatrix}$$

and $D = [\mathbf{0}_{4 \times 4}]$.

IV. ITERATIVE LQR CONTROLLER

The purpose of this report is to develop an iterative LQR optimal controller. This method uses iterative linearisation of the non-linear dynamic model and cost function around the **nominal optimal requirement result**. The discrete-time non-linear dynamical model is

$$x_{k+1} = f(x_k, u_k). \quad (22)$$

The quadratic form cost function is

$$J = \frac{1}{2}(x_N - x^*)'Q_f(x_N - x^*) + \frac{1}{2} \sum_{k=0}^{N-1} (x_k'Qx_k + u_k'Ru_k). \quad (23)$$

The iterative LQR method starts with a nominal control sequence and a **corresponding trajectory represented by x_k and u_k** , respectively. The nominal state is acquired from applying u_k to the open loop dynamical model iteratively. Through this iteration, the improved sequence u_k is obtained by linearising the dynamics of the system around control u_k and state x_k . Then the modified LQR problem is solved and convergence is achieved by keeping refined iteration due to the deviation of control δu_k and state δx_k from the nominal [14][15]. The linearisation system is

$$\delta x_{k+1} = A_k \delta x_k + B_k \delta u_k. \quad (24)$$

The **Hamiltonian function** is a first step to proceed with the optimal control δu_k represented as:

$$\begin{aligned} H_k &= (x_k + \delta x_k)'Q(x_k + \delta x_k) \\ &\quad + (u_k + \delta u_k)'R(u_k + \delta u_k) \\ &\quad + \lambda_{k+1}'(A_k \delta x_k + B_k \delta u_k). \end{aligned} \quad (25)$$

The required derivatives of the Hamiltonian function according to the minimum improvement of value Equation (25) are:

$$\frac{\partial H_k}{\partial(\delta x_k)} = \lambda_k, \frac{\partial H_k}{\partial(\delta u_k)} = 0, \frac{\partial H_k}{\partial(\delta x_N)} = \lambda_N. \quad (26)$$

The optimal control error equation is presented as:

$$\delta u_k = -K \delta x_k - K_v v_{k+1} - K_u u_k. \quad (27)$$

The thrust and torque control error equations for the system are considered in the following:

$$\delta F_k = -K \delta z_k - K_v v_{k+1} - K_F u_F \quad (28)$$

$$\delta M_k = -K \delta X_k - K_v v_{k+1} - K_M M_k \quad (29)$$

Consequently,

$$K = (B_k' S_{k+1} B_k + R)^{-1} B_k' S_{k+1} A_k \quad (30)$$

$$K_v = (B_k' S_{k+1} B_k + R)^{-1} B_k' \quad (31)$$

Symbol	Definition	Value	Units
I_x	Roll Inertia	4.4×10^{-3}	$kg.m^2$
I_y	Pitch Inertia	4.4×10^{-3}	$kg.m^2$
I_z	Yaw Inertia	8.8×10^{-3}	$kg.m^2$
m_Q	Mass	0.5	kg
m_L	Mass	0.2	kg
g	Gravity	9.81	m/s^2
l	Arm Length	0.17	m
L	Cable Length	1	m
I_r	Rotor Inertia	4.4×10^{-5}	$kg.m^2$

TABLE I
QUADROTOR PARAMETERS

$$K_u = (B_k' S_{k+1} B_k + R)^{-1} R. \quad (32)$$

The **backward recursion equations** which are used to solve the entire sequences S_k and v_k are

$$S_k = A_k' S_{k+1} (A_k - B_k K) + Q \quad (33)$$

$$v_k = (A_k - B_k K)' v_{k+1} - K' R u_k + Q x_k \quad (34)$$

where the gains K and K_u rely on the **Riccati equation** while the gain K_v is reliant on auxiliary sequence (34).

The improved control sequence originates from the summation of the nominal control and the three terms of control derivation for thrust and tours [16] shown as:

$$F_k^* = F_k + \delta F_k \quad (35)$$

$$M_k^* = M_k + \delta M_k. \quad (36)$$

Two paths have been introduced to control quadrotor-load positions and orientations using iLQR control, where the payload weight is 500g. The first desired path is tracked by a quadrotor carrying a load and presented by $x = 1, y = 1$ and $z = 2$, while a spiral trajectory is presented as a second desired path for the system according to the directions $x = 0.5 * \sin(\text{time}/2), y = 0.5 * \cos(\text{time}/2)$ and $z = 1 + \text{time}/10$. The iLQR simulation results are illustrated in figures with multi-iterations for two trajectories and are then compared with the results of the LQR controller, where the sampling time is 0.01 and the time consumption is 20 sec.

V. SIMULATION RESULTS

The proposed optimal controller ILQR is tested for a quadrotor with a slung load to improve stability in two paths using an MATLAB simulator, where the applied parameters for this simulation are shown in table I.

The iLQR controller does achieve lifting and transporting stability of the quadrotor with suspended payload. The test results are compared with those of the LQR optimal controller. In this simulation, the scenario is to control the four outputs parameters $Y = [x, y, z, \psi]$, reveal the desired states and then obtain the direction controllers x and y in order to find and control the attitude states ϕ_d, θ_d, ψ_d using the proposed controller.

LQR

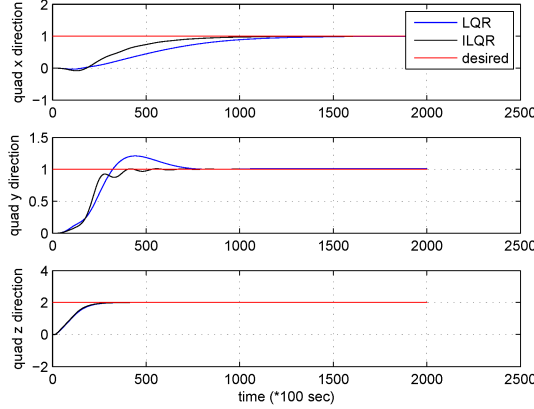


Fig. 1. Quadrotor actual position using LQR-ILQR controllers

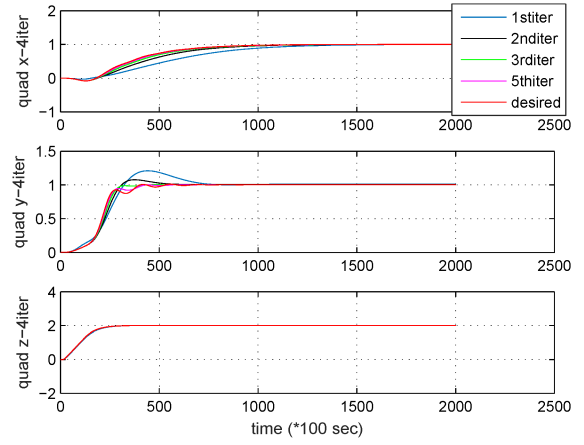


Fig. 2. Quadrotor actual position for 4 iterations using ILQR controller

The test results of the iLQR simulation control are presented by transporting the payload and tracking the two desired trajectories. The first step is to achieve hovering-transporting for the first trajectory. In the first scenario, the desired parameters for the quadrotor are comprised of altitude direction and rotation states $z_d = 2m$, $x_d = y_d = 0$, $\phi_d = \theta_d = \psi_d = 0$, while the load actual behaviour is approved to correspond the desired $z_{Ld} = 1m$, $x_{Ld} = y_{Ld} = 0$. Then the states of the final destination for the first trajectory are $z_d = 2m$, $x_d = y_d = 0$, $z_{Ld} = 1m$, $x_{Ld} = y_{Ld} = 0$ for the quadrotor and load positions as well quad orientations $\phi_d = \theta_d = \psi_d = 0$. The second scenario is implemented in simulation to track more aggressive trajectory to make the stability more challenging during the transporting task. A spiral trajectory is tested using the ILQR controller and the latter improves the accuracy of the quadrotor and load positions. In addition, it prevents load swing through model exchange and trajectory following in order to prove safe transportation for the load.

The performance of the first desired trajectory for the quadrotor and load are illustrated in Figures 1-5, where the position performance comparison between the LQR and the iLQR controllers with respect to the desired trajectory of the quadrotor and load are shown in Figures 1 and 4. The position performance of each iteration for the quadrotor and load are shown in Figures 2 and 5, while the quad attitude simulation test is described in Figure 3. In the other scenario, the second trajectory is presented by Figures 6 for quad position along the spiral path and 7 for load stability. Both trajectories results show improvement in performance with small steady state errors.

According to these results, the performance of the iLQR controller was faster with a smaller steady state error than that of the LQR controller. In both trajectories, the result of the iLQR controller is better than that of the LQR controller in terms of the cost function, steady state error and time-consumption.

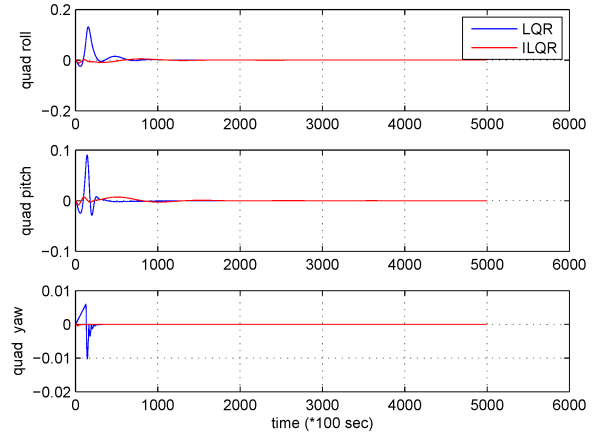


Fig. 3. Quadrotor angles using IQR-ILQR controllers

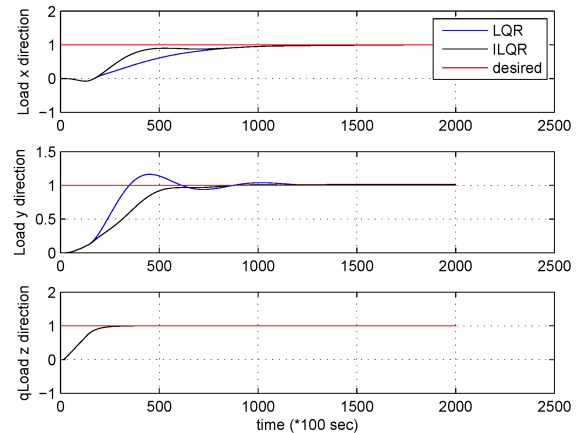


Fig. 4. Qudrotor transporting for step trajectory using LQR and ILQR Controllers

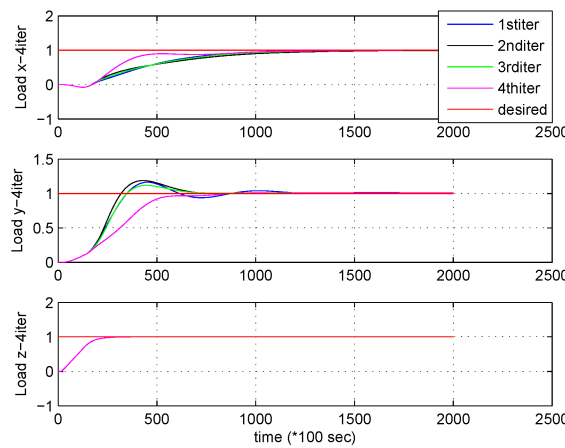


Fig. 5. Load position for step trajectory using LQR and ILQR Controllers

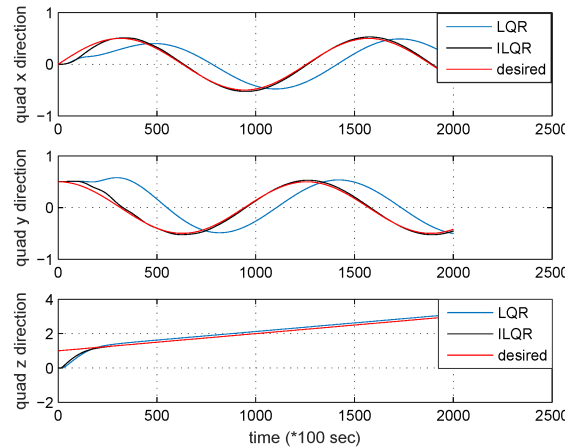


Fig. 6. Quadrotor position for spiral trajectory using LQR and ILQR Controllers

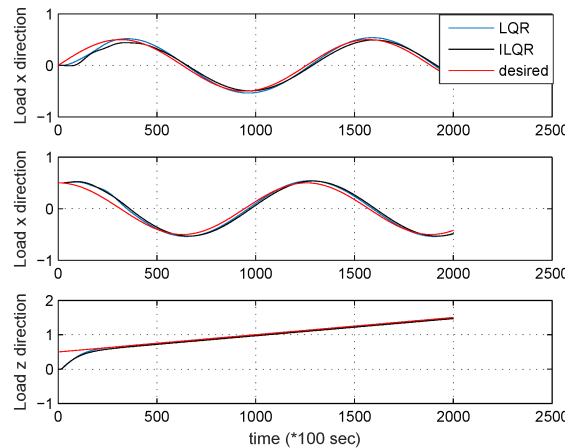


Fig. 7. Load position using LQR and ILQR Controllers

VI. CONCLUSIONS

This paper proposes an iLQR optimal controller for quadrotor flight control with a cable-suspended load. The iLQR control approach was developed based on the LQR controller. The proposed controller was tested in simulation and the result shows its ability to control the quadrotor and the suspended load. For comparison purposes, the LQR controller was tested in simulation as well. Our next step work along this direction is to use more than one quadrotor to lift and transport one load.

REFERENCES

- [1] S. Sadr, S. A. A. Moosavian, and P. Zarafshan, "Dynamics modeling and control of a quadrotor with swing load," *Journal of Robotics*, vol. 2014, 2014.
- [2] K. Sreenath, T. Lee, and V. Kumar, "Geometric control and differential flatness of a quadrotor UAV with a cable-suspended load," in *Decision and Control (CDC), 2013 IEEE 52nd Annual Conference on*, pp. 2269–2274, IEEE, 2013.
- [3] K. Klausen, T. I. Fossen, and T. A. Johansen, "Nonlinear control of a multirotor uav with suspended load," in *Unmanned Aircraft Systems (ICUAS), 2015 International Conference on*, pp. 176–184, IEEE, 2015.
- [4] J. E. Trachte, L. F. Gonzalez Toro, and A. McFadyen, "Multi-rotor with suspended load: System dynamics and control toolbox," in *Aerospace Conference, 2015 IEEE*, pp. 1–9, IEEE, 2015.
- [5] F. Gonzalez, A. Heckmann, S. Notter, M. Zürn, J. Trachte, and A. McFadyen, "Non-linear model predictive control for uavs with slung/swung load," 2015.
- [6] B.-Y. Lee, S.-M. Hong, D.-W. Yoo, H.-I. Lee, G.-H. Moon, and M.-J. Tahk, "Design of a neural network controller for a slung-load system lifted by 1 quad-rotor," *Journal of Automation and Control Engineering Vol.*, vol. 3, no. 1, 2015.
- [7] S. Tang and V. Kumar, "Mixed integer quadratic program trajectory generation for a quadrotor with a cable-suspended payload," in *Robotics and Automation (ICRA), 2015 IEEE International Conference on*, pp. 2216–2222, IEEE, 2015.
- [8] P. Cruz and R. Fierro, "Autonomous lift of a cable-suspended load by an unmanned aerial robot," in *Control Applications (CCA), 2014 IEEE Conference on*, pp. 802–807, IEEE, 2014.
- [9] C. Raimúndez and J. L. Camañ, "Transporting hanging loads using a scale quad-rotor," in *CONTROLO2014—Proceedings of the 11th Portuguese Conference on Automatic Control*, pp. 471–482, Springer, 2015.
- [10] Y. Alothman, W. Jasim, and D. Gu, "Quad-rotor lifting-transporting cable-suspended payloads control," in *Automation and Computing (ICAC), 2015 21st International Conference on*, pp. 1–6, IEEE, 2015.
- [11] M. W. Mueller and R. D'Andrea, "Stability and control of a quadcopter despite the complete loss of one, two, or three propellers," in *Robotics and Automation (ICRA), 2014 IEEE International Conference on*, pp. 45–52, IEEE, 2014.
- [12] C. de Crouzaz, F. Farshidian, M. Neunert, and J. Buchli, "Unified motion control for dynamic quadrotor maneuvers demonstrated on slung load and rotor failure tasks," in *Robotics and Automation (ICRA), 2015 IEEE International Conference on*, pp. 2223–2229, IEEE, 2015.
- [13] C. de Crouzaz, F. Farshidian, and J. Buchli, "Aggressive optimal control for agile flight with a slung load," in *IEEE/RSJ International Conference on Intelligent Robots and Systems (IROS) Workshop on Machine Learning in Planning and Control of Robot Motion*, 2014.
- [14] W. Li and E. Todorov, "Iterative linear quadratic regulator design for nonlinear biological movement systems," in *ICINCO (1)*, pp. 222–229, 2004.
- [15] H.-j. Zhang, J.-w. Gong, Y. Jiang, G.-m. Xiong, and H.-y. Chen, "An iterative linear quadratic regulator based trajectory tracking controller for wheeled mobile robot," *Journal of Zhejiang University SCIENCE C*, vol. 13, no. 8, pp. 593–600, 2012.
- [16] J. van den Berg, "Iterated lqr smoothing for locally-optimal feedback control of systems with non-linear dynamics and non-quadratic cost," in *American Control Conference (ACC), 2014*, pp. 1912–1918, IEEE, 2014.